Defence Science Journal, Vol. 61, No. 2, March 2011, pp. 180-190, DOI: 10.14429/dsj.61.477
© 2011, DESIDOC

Aluminide Coatings on Titanium-based Alloy IMI-834 for High Temperature Oxidation Protection

Md. Zafir Alam*, and Dipak K. Das

Defence Metallurgical Research Laboratory, Hyderabad–500 058
E-mail: zafir@dmrl.drdo.in, dkdas@dmrl.drdo.in

ABSTRACT

Microstructural aspects and cyclic oxidation behaviour of plain aluminide and *Pt*-aluminide coatings on the near-α *Ti*-alloy IMI-834 have been studied. Both the coatings provide good oxidation resistance to the above alloy at 650 °C, 750 °C, and 850 °C. However, significant cracking develops in the coatings during coating formation as well as during cyclic oxidation exposure. The extent of cracking during oxidation is found to increase with the exposure temperature. Presence of through-thickness cracks in the coatings leads to localised oxidation damage of the underlying substrate at all the three temperatures. At 850 °C, such localised oxidation generates enough TiO_2 so that this oxide phase grows through the cracks and emerges at the sample surface forming a clearly identifiable mud-crack pattern. The extent of such oxidation damage is comparatively much lower at 750 °C and 650 °C.

Keywords: Coatings, oxidation, titanium, IMI-834 alloy, near-alpha titanium alloy, aluminide, Pt-aluminide, aluminide coatings

1. INTRODUCTION

Titanium and its alloys offer designers several attractive properties such as exceptional corrosion resistance and high specific strength. However, their utilisation has been restricted because of certain inherent shortcomings associated with these materials such as poor high temperature oxidation resistance, susceptibility to adhesive and fretting wear, and poor galvanic compatibility with less corrosion-resistant materials. High temperature oxidation is currently proving to be a stumbling block for the use of near-α *Ti*-alloys such as IMI-834, IMI-829, and TIMETAL 1100. Prolonged oxidation exposure of the above alloys at high temperatures (above ~500 °C) is known to cause the formation of a brittle α casing which undermines the mechanical properties of these alloys[1]. Therefore, several coatings including *TiAlN*, Al_3Ti-type aluminide, silicide and MCr*Al*Y (M=*Ni*, *Co* or *Fe* or a combination of these elements)[2-8] are being examined for providing oxidation protection to the near-α alloys in the temperature range of 600-750°C.

The IMI-834 alloy is currently being used for compressor parts in modern gas turbine engines. The maximum temperature of use for this alloy is approximately 650°C and to protect this alloy from oxidation damage during application, several coatings have been reportedly used including some of those listed above. Diffusion aluminide coatings of the type Al_3Ti (or plain aluminide coating, as it is often called) and *Pt*-aluminide have been reported to offer very good oxidation resistance to IMI-834 alloy[3, 9-11]. Nicholls, *et al.*[10] and, more recently, Gurrappa and Gogia[11] have reported that *Pt*-aluminide coating can protect IMI-834 alloy from oxidation damage over long-term exposure at high temperatures up to 800 °C. They have also shown the superiority in oxidation resistance of *Pt*-aluminide coating over its plain aluminide counterpart in air at 800 °C. Despite these studies, the microstructural aspects of aluminide coatings on near-α *Ti* alloys have not been reported well. Further, oxidation performance of coated IMI-834 alloy, as reported by Gurappa and Gogia, has been evaluated under isothermal conditions. The performance under cyclic heating and cooling, which is practically more relevant, has not been reported. In the present study, detailed microstructural characterisation of a plain aluminide coating and a *Pt*-aluminide coating formed on IMI-834 alloy using the pack aluminising method has been carried out. These coatings have also been evaluated for their cyclic oxidation performance in air at three temperatures, namely 650 °C, 750 °C, and 850 °C. Microstructural degradation in the coatings as well as the evolution of the coating surface during oxidation have also been investigated. The reason for testing at temperatures higher than the maximum useful temperature of 650 °C for the alloy, i.e., at 750 °C and 850 °C, was to accelerate the oxidation-induced degradation process in the coatings, which otherwise would take extremely long exposures to generate at 650 °C.

2. EXPERIMENTAL DETAILS

The IMI-834 alloy, which was used as substrate in the present study, has a nominal composition as mentioned in Table 1. The β transus temperature, i.e., the temperature at which the α→β transformation takes place, of this alloy

Received 5 July 2010, Revised 26 October 2010, Published Online 13 February 2011

Table 1. Nominal composition (Wt.%) of IMI-834 alloy used in the present study

Al	*Sn*	*Zr*	*Nb*	*Mo*	*Si*	*C*	*Fe*	*O* (ppm)	*N* (ppm)	*H* (ppm)
5.8	4.0	4.0	0.75	0.50	0.4	0.06	0.05	1000	1500	60

was 1055 °C. Forged IMI-834 rods of 20 mm diameter were obtained in fully heat-treated condition, i.e., solution treated at 1020 °C for 2 h followed by air cooling and subsequently aged at 700 °C for 2 h. In this condition, the alloy has the desired microstructure consisting of primary α and transformed β. The amount of primary α present in the heat treated alloy was approximately 15 vol. per cent. From these rods, disc samples of approximately 2 mm thickness were cut using wire EDM. These 20 mm dia and 2 mm thick disc samples were then used as substrates for coating formation.

The plain aluminide coating was deposited on these samples by a pack aluminisation process carried out at 700 °C for 6 h. For the formation of *Pt*-aluminide coating, a 2 µm thick *Pt* layer was first electrodeposited on the samples. The plated samples were given a diffusion heat treatment following which the pack aluminisation was carried out at 700 °C for 6 h. Subsequently, a post-aluminising heat treatment consisting of solutionising at 1020 °C for 2 h and aging at 700 °C for 2 h was given to the samples. The powder pack used for aluminising consisted of 15 Wt per cent of *Al*, 2 Wt per cent NH_4Cl, and balance calcined alumina powder. A flowing argon atmosphere was maintained throughout the diffusion and aluminising treatments, including cooling, to prevent oxidation of the samples. A flow diagram describing the method for the formation of aluminide coating on IMI-834 alloy has been presented in Fig. 1. Further details regarding the coating formation process can also be found[12,13]. Henceforth, the *Pt*-aluminide coating has been referred to as *PtAl* coating.

To assess the effectiveness of these coatings, cyclic oxidation of the IMI-834 alloy in bare, plain aluminide and

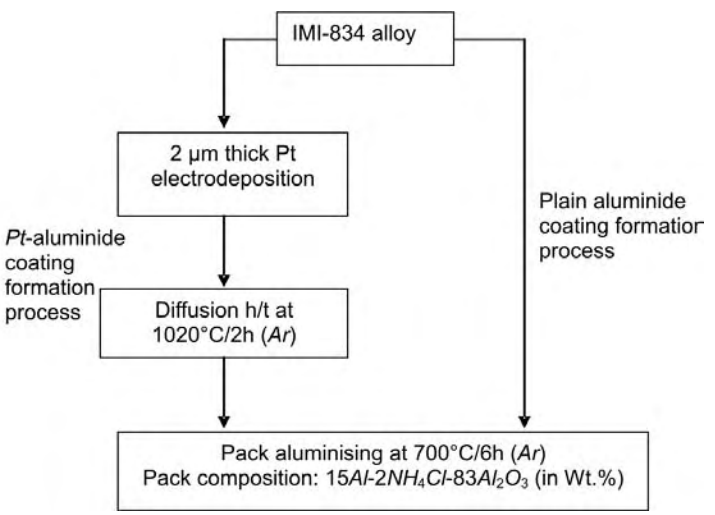

Figure 1. Schematic of the process for the development of *Pt*-aluminide and plain aluminide coatings on IMI-834 alloy.

Pt-aluminide coated conditions was conducted at 650 °C, 750 °C, and 850 °C in air. A cycle constituting of 0.5 h soaking at the designated test temperature followed by 0.5 h cooling in still atmospheric air was adopted for these oxidation tests. The cumulative exposure time at the high temperature was considered as the duration of oxidation for any sample. The cross-sections of the samples in both as-coated and oxidised conditions were metallographically mounted and polished for observation of the microstructure. A layer of nickel was electroplated on the samples prior to polishing to protect their edges during metallographic sample preparation. Microstructural study and related analyses were carried out using a scanning electron microscope and an electron probe micro-analyser (EPMA). The identification of phases in the coatings was carried out by x-ray diffraction (XRD) technique using $Cu\ K_a$ radiation.

3. RESULTS AND DISCUSSION

3.1 As-Formed Coating Microstructures

The microstructures of the as-formed plain aluminide and *PtAl* coatings are shown in Figs 2(a) and 2(b), respectively. The thickness of both the coatings was approximately 60 mm. As evident from Fig. 2(a), the plain aluminide coating has a single layer which consists of Al_3Ti phase. In case of *PtAl* coating [Fig. 2(b)], a three-layer structure is evident. The outer layer of this coating consists of $PtAl_2$ and Al_3Ti phases and the intermediate layer of Al_3Ti phase. The inner layer of the coating is the interdiffusion zone (IDZ), typically observed in all diffusion aluminide coatings[14-16]. Such three-layer microstructure of the *PtAl* coating has also been reported in case of *Ni*-based superalloy substrates, where β-*NiAl* rather than Al_3Ti phase is present along with $PtAl_2$ in the coating[16]. Further, unlike the precipitate-rich IDZ typically found in aluminide coatings on superalloys (see Fig. 3)[16,17], both plain aluminide (Fig. 2(a)) and *PtAl* [Fig. 2(b)] coatings on IMI-834 showed virtually no precipitates in the interdiffusion zone. *Ni*-based superalloys usually contain large of alloying additions in keeping with the requirements of high temperature mechanical properties. During the coating formation, *Ni* is depleted from the substrate due to its outward diffusion. Most of the alloying elements, which usually would remain in solid solution in the original γ-γ' structure of the substrate, precipitate out as complex phases after the loss of *Ni* because of their inadequate solubility in the resultant β-*NiAl* matrix of the IDZ[14,15]. In case of IMI-834, the total quantity of alloying elements is quite low at about 15 Wt. per cent (see Table 1) as compared to 50-60 Wt. per cent in superalloys. Because of such low alloying content of IMI-834, the alloying elements do not precipitate out in the IDZ despite the depletion of *Ti* from the substrate during coating formation. Further

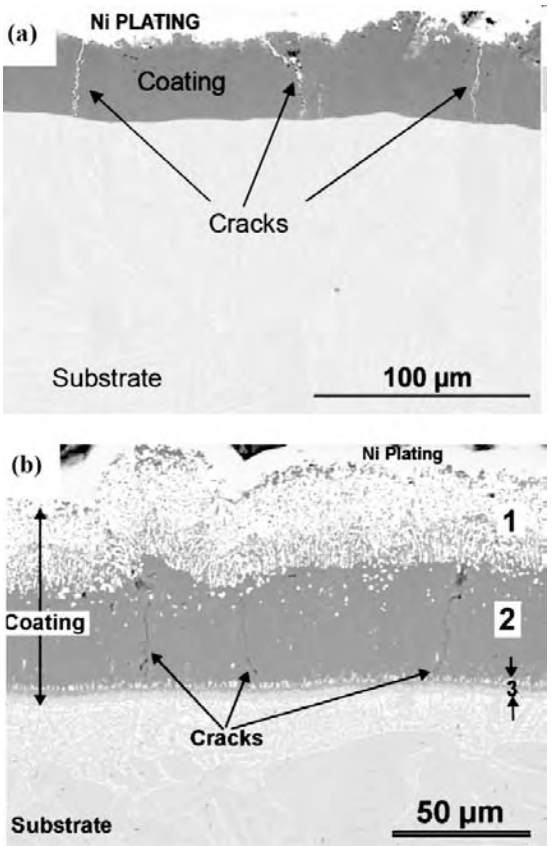

Figure2. Cross-sectional micrographs of as-formed coatings: (a) plain aluminide, and (b) *PtAl*. The three layers of the *PtAl* coating are marked as 1, 2, and 3.

details regarding the coating microstructures in case of IMI-834 alloy can be found[12,13].

Several through-thickness cracks were found in both the coatings, as indicated in Fig. 2. Such cracking of the coatings has been caused by the tensile stresses developed in the coating during cooling from aluminising temperature because of the difference in the coefficient of thermal expansion between the IMI-834 substrate and the Al_3Ti coating. Al_3Ti, being $D0_{22}$ in crystal structure, is known to have no ductility

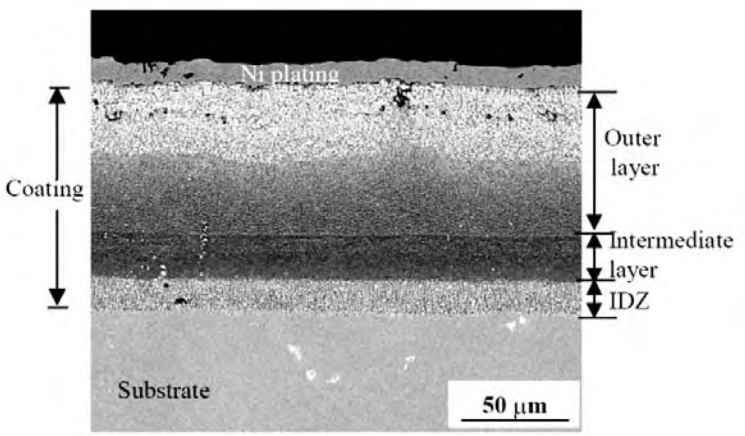

Figure 3. Microstructure of a typical *Pt*-aluminide coating on CM-247 LC DS alloy[16].

up to ~800 °C[18,19]. Therefore, this phase in the coating developed through thickness cracks for accommodating the above tensile stresses.

3.2 Cyclic Oxidation Performance

The weight-change plots for cyclic oxidation at 650 °C, 750 °C, and 850 °C for both the bare and the coated alloys are presented in Figs 4(a)-4(c). The bare alloy shows a gain in weight during the entire 500 h of oxidation at 650 °C. However, at higher temperatures of 750 °C and 850 °C, it loses weight after an initial period of weight gain. While the weight gain duration at 750 °C is about 250 h, it is 40 h at 850 °C (see Fig. 4). Unlike the bare alloy, the plain aluminide and the *Pt*-aluminide-coated samples exhibit weight gain during the entire durations of cyclic oxidation at all the three temperatures.

The parabolic oxidation rate constants (k_p) for the bare alloy and the aluminide-coated alloys are provided in Table 2. For comparison, the parabolic rate constant for α-*Ti*, as reported in the literature[20,21], has also been presented in the above table. The k_p values for the bare alloy corresponding to oxidation at 750 °C and 850°C were computed using only the weight gain data up to the point of maxima in the curves shown in Fig. 4. From Table 2, it is evident that the IMI-834 alloy is nearly twice and 25-times more oxidation-resistant than α-*Ti* at 750 °C and 850°C, respectively. From the Arrhenius equation, i.e. $k_p = k_0\, e^{-(E/RT)}$, where k_0 is the pre-exponential factor, E the activation energy for oxidation, R the universal gas constant and T the oxidation temperature in K, the value of E can be determined from the plot ln (k_p) vs. $1/T$[22]. The activation energy E for oxidation in the present case of bare IMI-834 alloy is calculated to be 43.9 kCal mole^{-1}. This value agrees well with the reported values of 40-50 kCal mole^{-1} for α-*Ti*[20,21].

the near-α *Ti*-alloys have been reported to have poor oxidation resistance in air above about 600 °C. Apart from developing a non-protective TiO_2 scale during oxidation, these alloys also form a brittle α-*Ti* casing on the surface due to the dissolution of oxygen in the alloy during the high temperature exposure[1,2,8]. Such a casing causes degradation of the mechanical properties of these alloys[1,2,8]. As mentioned before, IMI-834 alloy, like most *Ti*-alloys, forms a TiO_2 scale at all three oxidation temperatures. As a result, the parabolic oxidation would be controlled by the diffusion of the oxidising species (oxygen and/or *Ti* ions[20-23]) through

Table 2. Comparison of parabolic rate constant k_p values (in g^2 cm^{-4} s^{-1}) for bare and aluminide-coated IMI-834 alloy as a function of cyclic oxidation temperature[20,21].

Sample Type	650 °C	750 °C	850 °C
Bare	2.64 x 10^{-13}	4.92 x 10^{-12}	1.82 x 10^{-11}
Plain aluminide	3.16 x 10^{-14}	2.53 x 10^{-13}	6.1 x 10^{-12}
PtAl	1.16 x 10^{-14}	6.46 x 10^{-14}	2.48 x 10^{-12}
α-*Ti*	---	1.04 x 10^{-11}	4.28 x 10^{-10}

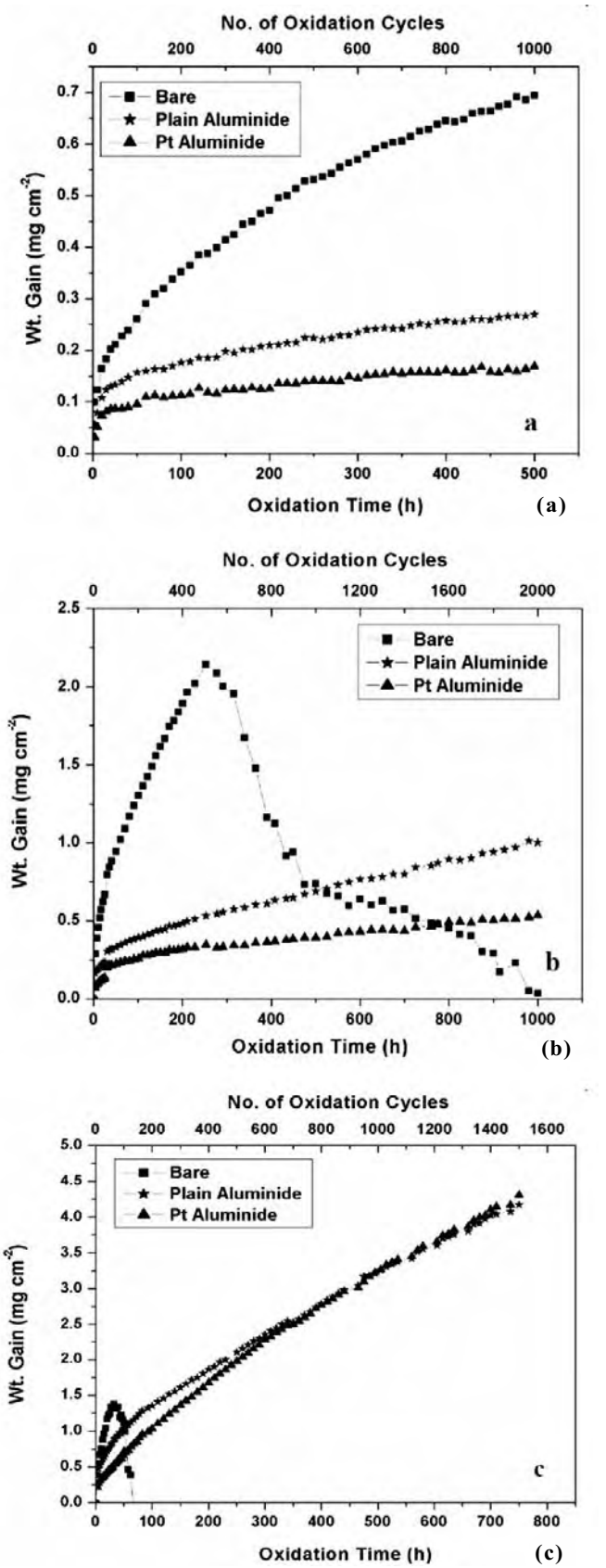

Figure 4. Comparative cyclic oxidation plots for bare and aluminide coated IMI-834 alloy at (a) 650 °C, (b) 750 °C and (c) 850 °C.

the TiO_2 scale. The activation energy of 43.9 kCal mole^{-1} calculated for this alloy, therefore, corresponds to the activation energy for the above diffusion process. Since the oxidation in case of α-*Ti* also occurs by the same mechanism, the activation energy for IMI-834 is found to be very similar to that for pure *Ti*. However, despite similar *E* values, the higher oxidation resistance of IMI-834 alloy as compared to α-*Ti* is believed to be due to the effect of various alloying elements, especially *Al*, in the alloy on the pre-exponential factor k_0 of the Arrhenius equation. Such case of rate getting affected through variation in pre-exponential factor, with activation energy remaining unchanged, has been reported in creep studies[24]. From the weight gain data (Fig 4(a) and 4(b)), this alloy seems to have a reasonably good cyclic oxidation resistance at 650 °C over the 1000 cycles (500 h) for which it was tested. However, its oxidation resistance degrades drastically at higher temperatures such as 750 °C and 850 °C (Figs. 4(b) and 4(c)), as indicated by much higher initial weight gain values followed by the loss in weight due to spallation of the TiO_2 scale (Fig. 5(b)). Based on the reported literature[1,8], the above alloy is expected to form the brittle α casing on the surface at all the three temperatures, although this aspect was not investigated in this study. Therefore, to enhance the oxidation resistance and to prevent the formation of a deleterious α-casing, IMI-834 alloy needs to be coated with an oxidation-resistant coating.

Applying an aluminide coating (either plain aluminide or *PtAl*) improves the oxidation resistance of IMI-834 alloy considerably, as evident from the weight change plots (Fig. 4) and the k_p values (Table 1). The oxidation rate for the coated alloy at 650 °C and 750 °C is 8-70 times lower than that of the bare alloy. At 850 °C, the coated alloy oxidises nearly 3-times slower than the bare IMI-834 alloy. The activation energy for oxidation for the plain aluminide and *PtAl* coatings are determined to be 53.6 kCal mole^{-1} and 54.4 kCal mole^{-1}, which are somewhat higher than that calculated for the bare alloy[20,21]. As evident from the weight change plots in Fig. 4, *PtAl* coating oxidises marginally slower than the plain aluminide coating at 650 °C and 750 °C. However, both the coatings are found to oxidise in a very similar manner at 850 °C (see Fig. 4). From the k_p values provided in Table 1, the oxidation rate of the *PtAl* coating is 2.5-4.0 times lower than that of its plain aluminide counterpart in the temperature range of 650 °C–850°C. Although the *PtAl* coating provides relatively better oxidation protection to IMI-834 alloy than the plain aluminide coating, it is unlike the case for *Ni*-based superalloy substrates where Pt-modified â-*NiAl* coating is known to provide far superior oxidation protection as compared to its plain aluminide counterpart[25-27]. For example, Das[27], *et al*. have reported that *PtAl* coating on superalloy CM-247LC provides 7.5-times better cyclic oxidation resistance than the plain aluminide coating at a temperature[27] as high as 1200 °C.

The improvement in the oxidation resistance in the coated alloy is due to the high *Al* containing Al_3Ti phase present in the coating, which enables the formation of a protective α-Al_2O_3 scale on the surface during oxidation

exposure[11,13]. However, since through-thickness cracks are present in these coatings, the activation energy of 53.6-54.3 kCal mole^{-1}, as determined for the coated alloy, would correspond to that for the combined diffusion of the oxidising species through the Al_2O_3 scale and through the cracks. Smialek[28], *et al*. have reported the oxidation behaviour of bulk Al_3Ti in the temperature range[28] of 600 °C–1300 °C. They observed that a protective α-Al_2O_3 scale forms at all temperatures in the above range. Therefore, the parabolic rate constants in the 1000 °C–1300°C range are small and comparable to those for the α-Al_2O_3 growth kinetics on β-*Ni*49*Al* and β-*Ni*42*Al* alloys. However, below 1000 °C, they observed the oxidation rate to increase with decrease in oxidation temperature. Further, an initial high oxidation rate followed by a much lower oxidation rate was also observed below 1000 °C. They ascribed such anomalous oxidation behaviour of bulk Al_3Ti below 1000 °C to the inhomogeneous microstructure of the Al_3Ti casting, which retained some amount of free *Al* as a non-equilibrium phase. Rapid internal oxidation of the *Al* phase, which is molten above 660 °C, was believed to cause an initial rapid rate of oxidation. After all the *Al* phase was completely oxidised, the oxidation rate decreased to that of the Al_3Ti. Above 1000 °C, they concluded that the anomalous oxidation was eliminated because of the quick homogenisation of the microstructure during oxidation exposure[28]. In the present case of plain aluminide coating, no such rapidly oxidising second phase was present and the coating had a single-phase Al_3Ti structure. The additional $PtAl_2$ phase present in the *PtAl* coating is also known to possess extremely good high temperature oxidation resistance based on the reported studies on *Pt*-aluminide coated Ni-base superalloys[14,15,17]. Therefore, unlike in the case[28] of bulk Al_3Ti, a normal behaviour of oxidation rate rising with increasing temperature was observed for both the above coatings on IMI-834 alloy (Table 2).

In case of β-*NiAl* coatings on *Ni*-based superalloys, oxidation protection is also achieved through the formation of an alumina scale. It has been widely reported that *Pt* addition to β-*NiAl* coatings improves their oxidation resistance significantly[25-27], although the exact mechanism by which *Pt* helps enhancing the oxidation resistance is not fully understood. It is believed that the presence of *Pt* increases the diffusivity of *Al* in the coating, which helps easy formation of the protective scale during oxidation[29,30]. Platinum is also thought to improve the oxidation resistance by lowering the growth stresses associated with the alumina scale[31-33] and enhancing the scale adherence with the substrate[34,35]. Although *Pt* can be expected to have similar effects in the case of Al_3Ti coatings, it, as mentioned earlier, does not lead to substantial increases in the oxidation resistance as reported for the *Pt*-modified β-*NiAl* coatings[25,27]. It can be speculated that the beneficial effect of *Pt* becomes more prominent only at much higher temperatures such as 1000 °C or above at which β-*NiAl* coatings are used. At lower temperatures such as 650 °C-850°C, as used in this study, the oxidation rates associated with the Al_3Ti coating are possibly too low to be greatly affected by the presence of *Pt*.

From the weight change data reported by Gurappa and Gogia[11] at 800 °C, the oxidation rate for the *PtAl* coating on IMI-834 can be calculated as 9.5x10^{-14} g^{2}cm^{-4}s^{-1}, which is nearly 58-times lower than the value of 5.5x10^{-12} g^{2}cm^{-4}s^{-1} for the plain aluminide coating. It is difficult in their study to guess how the *PtAl* coating was so superior to the plain aluminide coating, while it is found to be only 2.5-4.0 times better in the present study. It may not be prudent to compare our data with that of the above reported study for the following reasons:

- Firstly, Gurappa and Gogia have carried out oxidation under isothermal conditions, while it has been done under cyclic heating and cooling conditions in the present study. As it is well known, the oxidation rates under thermal cycling is usually much more severe than under isothermal conditions.
- Secondly, as would be shown later, oxidation in case of aluminide coatings on IMI-834 occurs both at the surface of the coating as well as underneath the through-thickness cracks present in the coating, where local oxidation of the substrate occurs. Thus, the weight gain value measured during oxidation is the combined effect of surface oxidation of the coating and localised oxidation of the underlying substrate.
- Gurappa and Gogia[11] have not made any mention of such coating cracks and their effect on the oxidation damage of the substrate.
- Additional studies need to be undertaken to understand the effect of *Pt* in enhancing the oxidation resistance of Al_3Ti coatings.

3.3 Surface Morphology after Oxidation

3.3.1 Bare Alloy

The surface morphology that develops on the bare alloy samples after oxidation at 650 °C and 750 °C is shown in Figs 5(a) and 5(b). The oxidised surface after 500 h at 650 °C (Fig. 5(a)) appears relatively damage-free as compared to the surface corresponding to 1000 h at 750 °C, where, large-scale spallation of the oxide scale is observed (Fig. 5(b)). Region 1, as marked in Fig. 5(b), shows a location where the oxide scale is sticking to the substrate, while Region 2 is the adjacent location from where the scale has spalled, exposing the underlying alloy. The EDS analysis of Region 1 (Fig. 5(c)) indicates the scale to be predominantly TiO_2 although *Al* was also detected along with *Ti* and *O*. The scale being TiO_2 was also confirmed by XRD study of the oxidised surface. The presence of all the substrate elements in Region 2 (Fig. 5(d)) confirms that the substrate has been exposed at this location because of the spallation of the oxide layer.

3.3.2 Coated Alloy

The surface morphology of *PtAl* coating in as-coated condition and after various durations of cyclic exposure at 750 °C is shown in Fig. 6. The through-thickness cracks present in the as-formed coating are barely visible on the

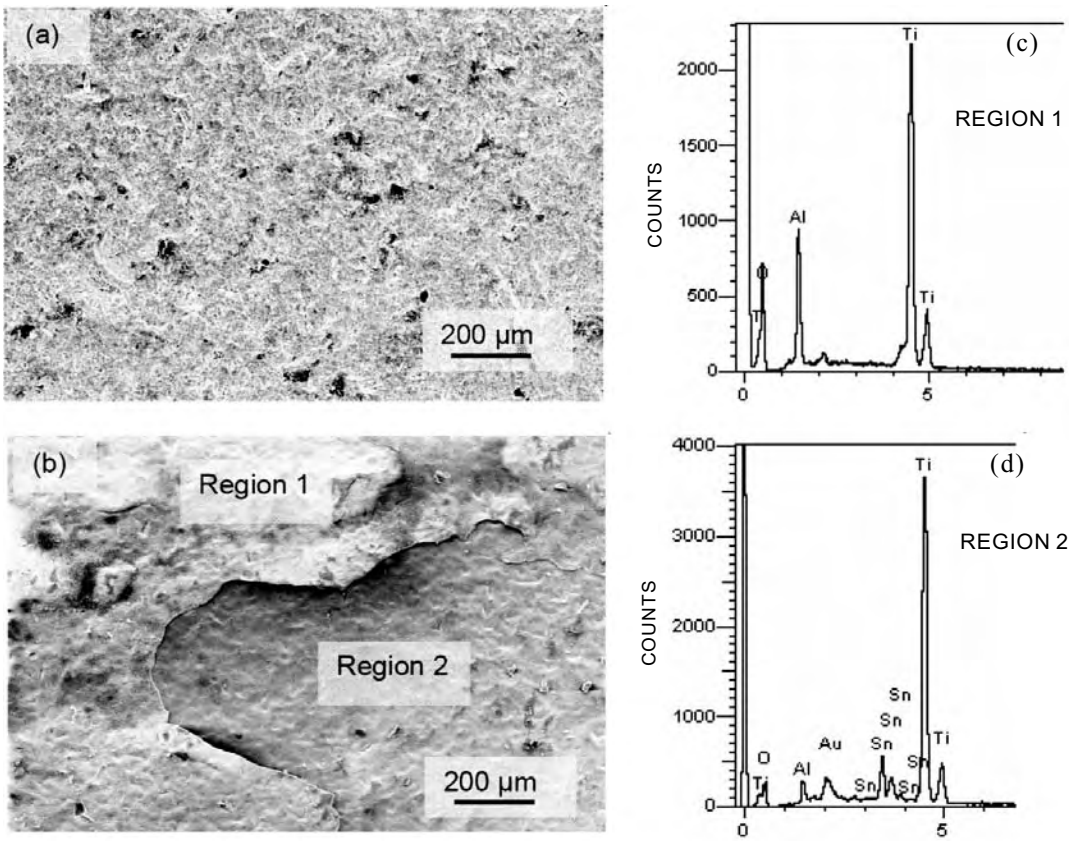

Figure 5. Surface morphology of bare IMI-834 alloy after cyclic oxidation: (a) 500 h at 650 °C and (b) 1000 h at 750 °C. The EDS plots taken on the oxidised surface at locations marked as: Region 1 and Region 2 are shown in (c) and (d), respectively.

surface in Fig. 6(a), although some of these cracks can be identified at higher magnifications. The coating develops further cracks during cycling at 750 °C. However, even after 2000 cycles (1000 h) at 750 °C, the cracks remain fairly fine and, therefore, are not very prominent at low magnifications (see in Fig. 6(b)), although these can be clearly seen at higher magnifications, as evident in Fig. 6(c). The oxidised surface corresponding to 750 °C exhibits a nodular morphology (Fig. 6(c)) and the scale is determined to be predominantly α-Al_2O_3, as evident in the EDS analysis in Fig. 6(d). The surface morphology and the nature of cracking in the case of oxidation at 650 °C is very similar to that described above for 750 °C and, therefore, has not been discussed separately.

Cyclic oxidation at 850 °C results in a very distinct mud-crack or segmented morphology on the coating surface, as seen in Fig. 7(a). The boundary regions of the segmented structure, which correspond to the cracks present in the coating, project out of the surface indicating comparatively larger oxide growth at these regions as compared to the rest of the surface. With the increase in number of cycles, further cracking in the coating takes place, increasing the boundary regions, as evident from Fig. 7(b). To estimate the extent of cracking with increase in the number thermal cycles, linear crack density (LCD) values were calculated for the as-coated as well as oxidised *PtAl*-coated samples. The LCD represents the number of cracks present per 1000 µm (1 mm) length on the coating surface. Table 2 presents the LCD values for *PtAl* coating. It is clear from the table that the extent of cracking increases with thermal cycling since the LCD value after cycling at any temperature is higher than that in the as-coated condition. Further, cycling at 850 °C leads to a considerably larger extent of cracking in the coating than that caused at either 650 °C or 750 °C. For example, LCD is 4.2 for 2000 cycles (1000 h) at 750 °C, while it is nearly double at 8.0 for 1500 cycles (750 h) at 850 °C.

Figure 7(c) presents the magnified view of a boundary region where it can be seen to consist of faceted grains which, based on the EDS analysis given in Fig. 7(d), are identified as TiO_2. The faceted grain morphology of the above oxide phase also indicates the phase to be rutile (TiO_2)[23]. Barring the boundary regions, the entire oxidised surface at 850 °C is covered with an alumina scale, as determined by EDS analysis as well as XRD study. Despite the gradual increase in cracking observed in the *PtAl* coating at all the three oxidation temperatures (Table 3), only in the case of oxidation at 850 °C, the TiO_2 oxide phase is found emerging through these cracks and protruding beyond the sample surface, forming the aforementioned mud-crack pattern. In fact, such a pattern develops gradually for the *PtAl* coating during cyclic oxidation at 850 °C, as evident

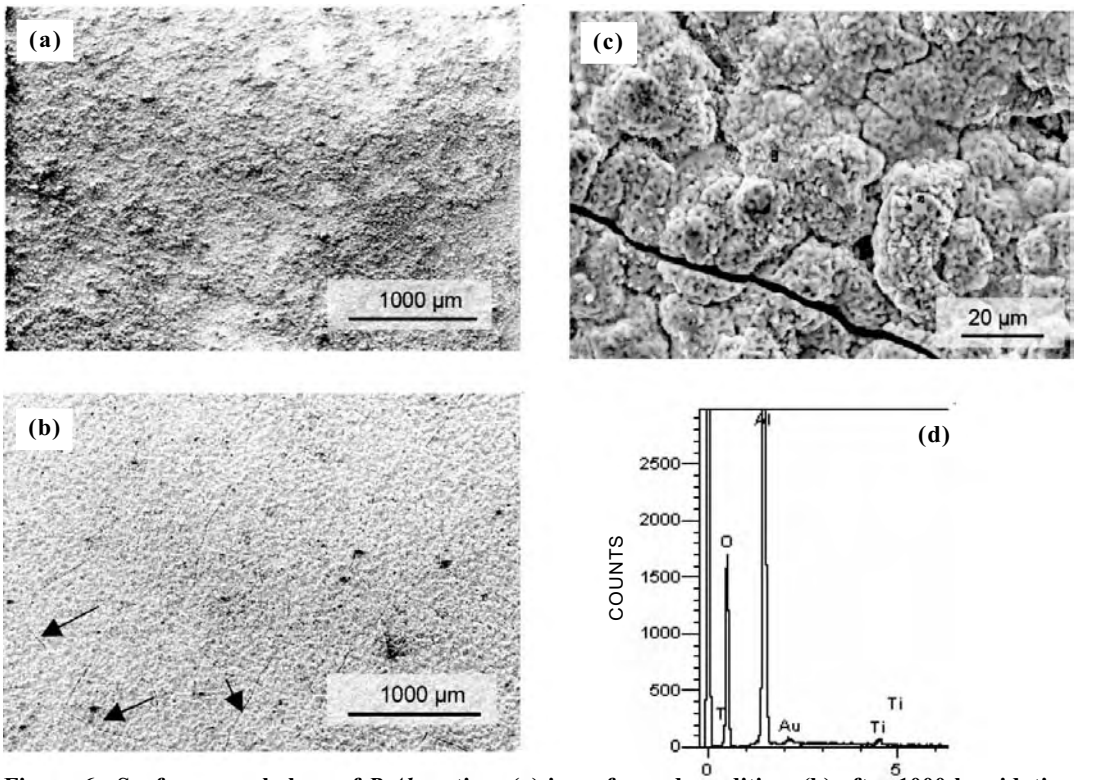

Figure 6. Surface morphology of *PtAl* coating: (a) in as-formed condition, (b) after 1000 h oxidation at 750 °C showing fine cracks (marked by arrows), (c) magnified view of the surface shown in (b) showing cracks and nodular morphology of the scale, and (d) EDS analysis of the surface shown in (c).

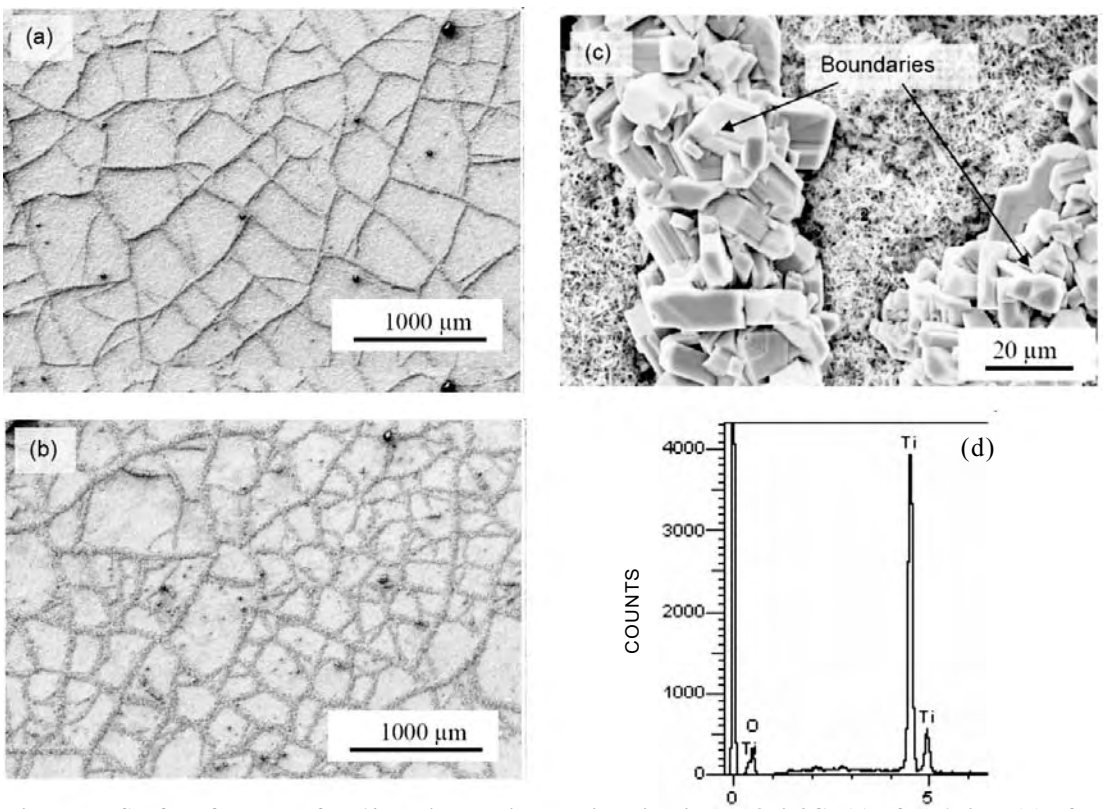

Figure 7. Surface features of *PtAl* coating during cyclic oxidation at 850 °C: (a) after 150 h, (b) after 750 h, (c) magnified view of the surface close to mud-cracks (formed after 750 h) showing the faceted outgrowth through the cracks, and (d) EDS pattern of the outgrowth indicating it to be TiO_2.

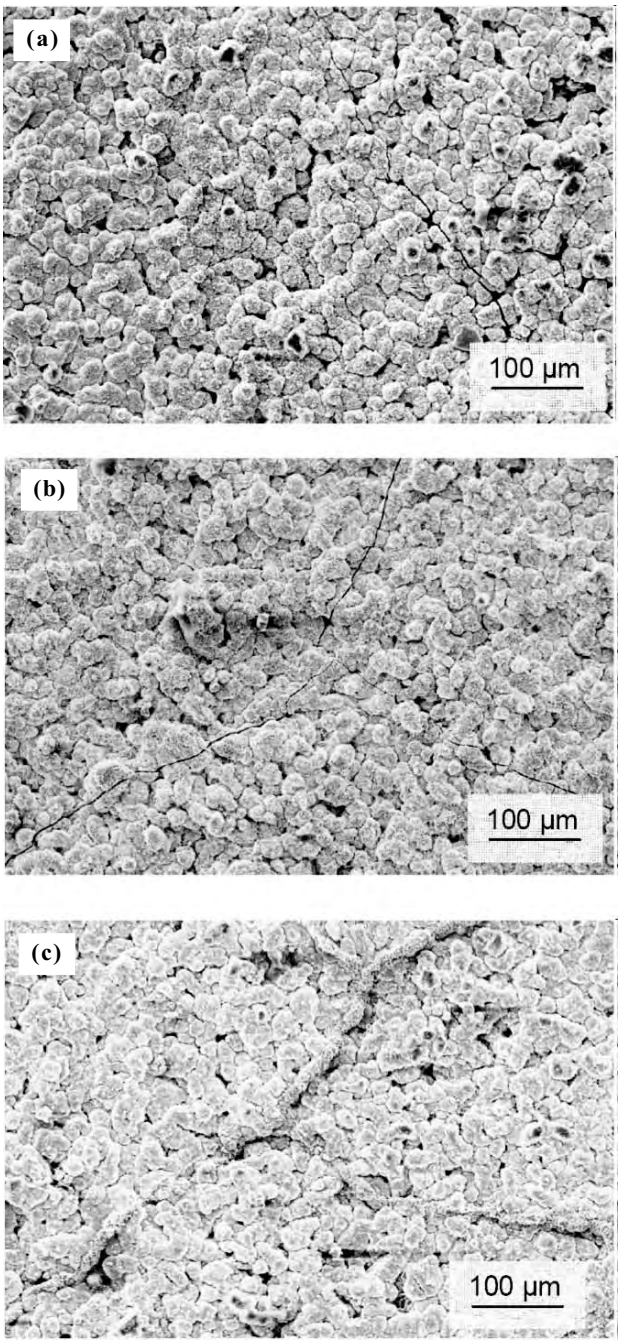

Figure 8. Surface morphology of *PtAl* coating during cyclic oxidation at 850 °C: (a) after 8 h and (b) 25 h, showing no outgrowths. However, after 50 h, the emanation and spread of TiO_2 outgrowth is seen, as shown in (c).

from the Fig. 8(a)-(c). After initial few cycles, the coating develops more cracking, as mentioned earlier, but without showing the presence of TiO_2 growth through the cracks (Figs 8(a) and 8(b)). After about 50 cycles, the mud-crack pattern becomes apparent on the coating surface with TiO_2 oxide phase emerging through the cracks (Fig. 8(c)). Beyond this time, a well-marked crack pattern continues to develop with further cracks getting added with the increase in the number of cycles. Eventually, the cracking and the crack pattern is expected to stabilise after a sufficiently large number of cycles. Oxidation at lower temperatures such as 650 °C and 750 °C also produces cracking in a similar manner as in the case of 850 °C, although to a much lesser extent (see Table 3). However, it does not result in a distinguishable mud-crack pattern because of adequate TiO_2 outgrowth through the cracks, even after long exposures (Fig. 6(c)). It may be noted that the evolution of surface morphology for the plain aluminide coating during oxidation is very similar to that mentioned above for the *PtAl* coating. The increased cracking in the plain aluminide coating with the rise in the number of cycles is evident from the LCD values mentioned in Table 2.

3.4 Coating Microstructure after Oxidation

It is observed that the microstructure of the coating does not undergo any appreciable change due to oxidation at all the three temperatures. This is evident from the cross-sectional microstructures of the *PtAl* coating corresponding to exposures at 750 °C and 850 °C, as shown in Figs 9 and 10, respectively. The starting three-layer structure of the coating had still remained after the prolonged exposure of 2000 cycles (1000 h) at 750 °C (Fig. 9) and 300 cycles (150 h) at 850 °C (Fig. 10). Localised oxidation of the underlying substrate through the cracks present in the coating occurs after exposure at all the temperatures, as typically seen in Figs 9 and 10. SEM-EDS analysis indicates that the oxide phase formed at the base of the crack is TiO_2 and that formed within the coating is primarily alumina. The extent of oxidation through the cracks at 850 °C is found to be much larger compared to that at 750 °C or 650 °C. This is evident from Fig. 10 where extensive oxidation at 850 °C has caused the formation of a large oxide mass inside the crack. The oxide mass seen at the top of the crack in Fig. 10(a) is actually the cross-sectional view of one of the boundaries in the mud-crack pattern that develops on the sample surface. Large scale localised oxidation of the substrate at the base of the crack can also be seen in Fig. 10. In case of plain aluminide coating, similar oxide growth through the cracks, as mentioned above for the *PtAl* coating, is also observed.

Despite the good oxidation resistance provided by the aluminide coatings to IMI-834 alloy, the extreme brittleness of these coatings make them prone to cracking under CTE mismatch stresses. The through-thickness cracks initiate during coating formation (Fig. 2) and their numbers grow during thermal cycling (Table 3) as more mismatch stresses are generated with each additional cycle. The cracks provide a passageway for the atmospheric air to come in direct contact with the unprotected substrate below the coating, leading to localised oxidation at the base of the cracks. Therefore, the presence of the cracks prevents the aluminide coatings from providing complete oxidation protection to the underlying substrate. This aspect, however, is not apparent from the weight change data (Fig. 4).

The IMI-834 alloy is designed for long-term use at a maximum temperature of about 650°C. By carrying out oxidation

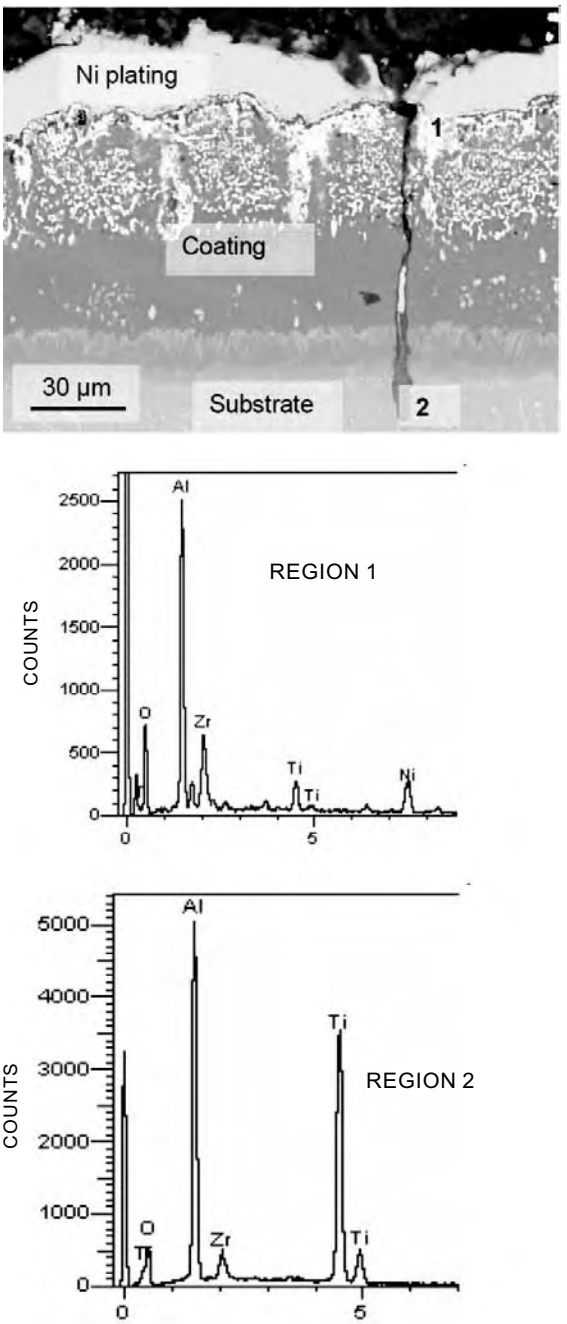

Figure 9. Localised oxidation beneath a through-thickness crack in *PtAl* coating. The coating was subjected to cyclic oxidation at 750 °C for 1000 h. The EDS plots for the regions 1 and 2 are provided.

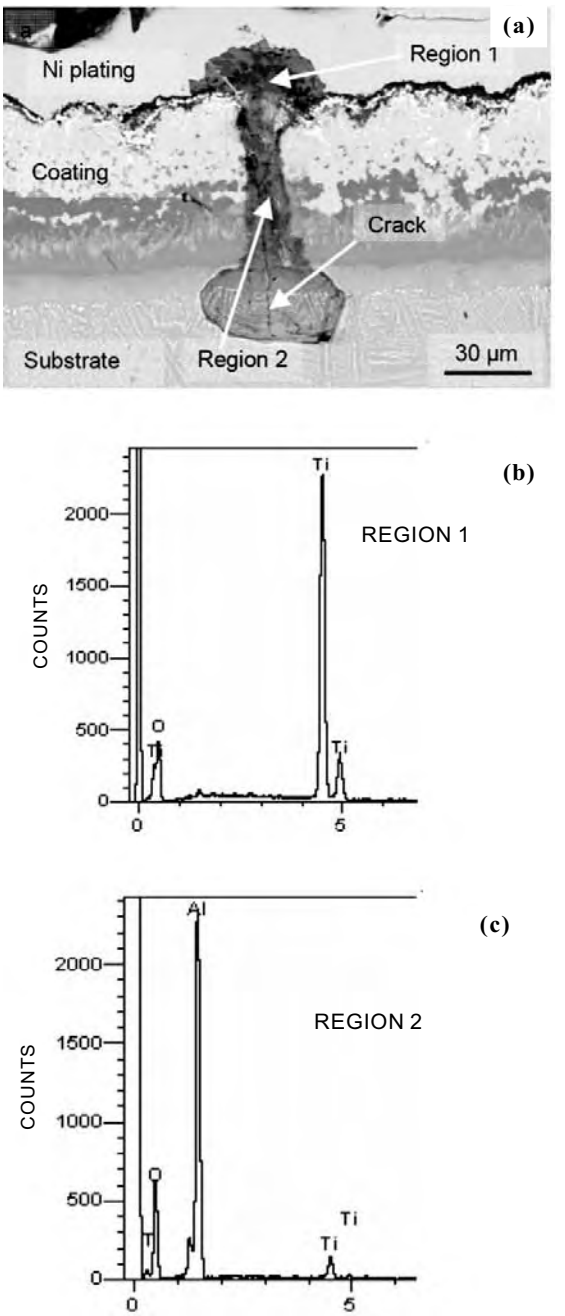

Figure 10. (a) Cross section view of the *PtAl* coating after 150 h of cyclic oxidation at 850 °C showing localised degradation along a through-thickness crack, (b) EDS pattern indicating the presence of TiO_2 in the top regions of the crack, and (c) EDS pattern showing the presence of both alumina and TiO_2 in the lower regions of the crack.

at higher temperatures such as 750 °C and 850°C, the oxidation process has been accelerated to generate damages that, otherwise, would take extremely long exposures to generate at 650 °C. Although a significantly high localised oxidation damage to the substrate is caused by cyclic exposure at 850 °C, the damage caused at 750 °C and 650 °C is found to be comparatively much less even after prolonged exposures of > 1000 h (2000 cycles). Further, the large scale outgrowth of TiO_2 through the cracks leading to the formation of the mud-crack pattern is absent at 750 °C and 650 °C [Fig. 6(c)]. Therefore, it can be concluded that the oxidation process for the aluminide-coated IMI-834 alloy is fairly slow at temperatures below 750 °C, and it would probably take an extremely long time, may be several thousands of hours of exposure, at these temperatures to develop the mud-crack morphology, as observed at 850 °C.

It is known that intermetallic-based coatings degrade the mechanical properties of the substrate alloy[36]. Therefore, Al_3Ti type coatings can also be expected to have similar

effects on the mechanical properties of IMI-834 alloy. Generation of through-thickness cracks in these coatings during application can potentially cause further deterioration of the mechanical properties. Therefore, it is important to weigh the beneficial effects of these coatings in terms of their ability to improve the oxidation resistance against their propensity to cause degradation in the mechanical properties of the substrate alloy.

4. CONCLUSIONS

In this study, microstructural aspects and cyclic oxidation performance (at 650 °C, 750 °C, and 850 °C) of plain aluminide and *Pt*-aluminide coatings on near-α *Ti*-alloy IMI-834 have been reported. Both these coatings provide good oxidation resistance to IMI-834 at all the three temperatures. However, these develop through-thickness cracks under the influence of CTE mismatch stresses during the coating formation as well as during thermal cycling. The number of cracks in the coating increases with the number of thermal cycles at any given temperature, although the increase is the highest in case of cycling at 850 °C. Presence of the cracks in the coating leads to localised oxidation damage in the underlying substrate. Localised oxidation at 850 °C occurs at a rapid rate and generates enough TiO_2 which grows outward through the cracks to emerge on the sample surface in the form of a prominent mud-crack pattern. The extent of oxidation damage is comparatively much lower at 750 °C and 650°C.

ACKNOWLEDGEMENTS

The authors acknowledge the assistance provided by the XRD, SEM and EPMA groups of Defence Metallurgical Research Laboratory for characterisation of the coatings. They are thankful to Director, DMRL, for his permission to publish the present work which was sponsored by the Defence Research and Development Organisation.

REFERENCES

1. Leyens, C. Titanium and titanium alloys, edited by C. Leyens and M. Peters. Wiley-VCH, Weinheim, 2003, 187p.
2. Krac, J.; Ferdinandy, M.; Liska, D. & Tuleja, S. *In* Conference Proceedings on High Temperature Intermetallics, London, UK, 30 Apr.-1 May, 1991, The Institute of Metals, London, 1991. pp. 191-93.
3. Dewald, D.K. & Mikkola, D.E. *In* Conference Proceedings on Elevated Temperature Coatings: Science and Technology II, Anaheim, California, USA, 4-8 Feb. 1996, Minerals, Metals and Materials Society/AIME, Warrendale, PA, 1996. pp. 255-264.
4. Takei, A. & Ishida, A. *In* Conference Proceedings on High Temperature Corrosion of Advanced Materials and Protective Coatings, Tokyo, Japan, 5-7 Dec. 1990, Elsevier Science Publishers B.V., Sara Burgerhartstraat, Amsterdam, 1992. pp. 317-324.
5. McMordie, B.G. Oxidation resistance of slurry aluminides on high temperature titanium alloys. *Surf. Coat. Technol.,* 1991, 49(1-3), 18-23.
6. Cockeram, B.V. & Rapp, R.A. Isothermal and cyclic oxidation resistance of boron-modified and germanium-doped suicide coatings for titanium alloys. *Oxidation Metals*, 1996, **45**(5-6), 427-68.
7. Cockeram, B.V. & Rapp, R.A. The kinetics of multilayered Titanium-Silicide coatings grown by the pack cementation method. *Metall. Mater. Trans. A*, 1995, **26**A, 777-91.
8. Leyens, C.; Peters, M. & Kaysser, W.A. *In* Titanium '99: Science and Technology, St. Petersberg, Russia, 1999. pp. 866-75.
9. Brady, M.P. & Tortorelli, P.F. Alloy design of intermetallics for protective scale formation and for use as precursors for complex ceramic phase surfaces. *Intermetallics*, 2004, **12**(7-9), 779-89.
10. Nicholls, J.R.; Winstone, M.R.; Deakin, M.J. & Kerry, S. *In* Conference Proceedings on Elevated Temperature Coatings: Science and Technology II, Anaheim, California, USA, 4-8 Feb. 1996, Minerals, Metals and Materials Society/AIME, Warrendale, PA, 1996. pp. 199-208.
11. Gurrappa, I. & Gogia, A.K. Development of oxidation resistant coatings for titanium alloys. *Mater. Sci. Technol.*, 2001, **17**(5), 581-87.
12. Trivedi, S.P. & Das, D.K. Microstructural aspects of plain aluminide and Pt-aluminide coatings on Ti-base alloy IMI-834. *Intermetallics*, 2005, **13**(10), 1122-133.
13. Das, D.K. & Trivedi, S.P. Microstructure of diffusion aluminide coatings on Ti-base alloy IMI-834 and their cyclic oxidation behaviour at 650 °C. *Mater. Sci. Eng. A*, 2004, **367**(1-2), 225-33.
14. Goward, G.W. & Boone, D.H. Mechanisms of formation of diffusion aluminide coatings on nickel-base superalloys. *Oxidation Metals*, 1971, **3**(5), 475-95.
15. Pichoir, R. Materials and coatings to resist high temperature corrosion, edited by D.R. Holmes and A. Rahmel, London, Applied Science Publishers, 1978. pp. 271-290.
16. Alam, M.Z.; Srivathsa, B.; Kamat, S.V.; Jayaram, V.; Hazari, N. & Das, D.K. Mechanism of failure in a free-standing Pt–aluminide bond coat during tensile testing at room temperature. *Mater. Sci. Eng. A*, 2010, **527**(3), 842-48.
17. Das, D.K.; Singh, V. & Joshi, S.V. Evolution of aluminide coating microstructure on nickel-base cast superalloy CM-247 in a single-step high-activity aluminizing process. *Metall. Mater. Trans. A*, 1998, **29**A, 2173-188.
18. Itoh, G.; Kita, K. & Kanno, M. *In* Titanium'95, Vol.-I, P.A. Blenkinsop, edited by W.J. Evans and H.M. Flower, The Institute of Materials, London, 1996. pp. 581-87.
19. Yamaguchi, M. & Umakoshi, Y. The deformation behaviour of intermetallic superlattice compounds. *Prog. Mater. Sci.*, 1990, **34**(1), 1-148.
20. Kofstad, P. High Temperature Corrosion, Elsevier Applied Science Publishers Ltd., 1988. 289p.
21. Kofstad, P. High-temperature oxidation of metals, John Wiley & Sons Inc., 1966. 169p.
22. Kofstad, P. High temperature corrosion, Elsevier Applied

Science Publishers Ltd., 1988. pp. 23-24.
23. Farrell, M.S.; Boone, D.H. & Streiff, R. Oxide adhesion and growth characteristics on platinum-modified aluminide coatings. *Surf. Coat. Technol.*, 1987, **32**(1-4), 69-84.
24. Mishra, R.S. & Banerjee, D. Microstructure and steady state creep in *Ti*-24*Al*-11*Nb*. *Mater. Sci. Eng. A*, 1990, **A130**(2), 151-64.
25. Sun, J.H.; Jang H.C. & Chang, E. Effects of pretreatments on structure and oxidation behaviour of d.c.-sputtered platinum aluminide coatings. *Surf. Coat. Technol.*, 1994, **64**(3), 195-203.
26. Das, D.K.; Roy M.; Singh, V. & Joshi, S.V. Microstructural degradation of plain and platinum aluminide coatings on superalloy CM247 during isothermal oxidation. *Mater. Sci. Technol.*, 1999, **15**(10), 1199-208.
27. Das, D.K.; Vakil Singh & Joshi, S.V. Effect of Al content on microstructure and cyclic oxidation performance of Pt-aluminide coatings. *Oxidation Metals*, 2002, **57**(3-4), 245-66.
28. Smialek, J.L. & Humphrey, D.L. Oxidation kinetics of cast $TiAl_3$. *Scripta Metall. Mater.,* 1992, **26**(1), 1763-768.
29. Krishna, G.R.; Das, D.K.; Singh, V. & Joshi, S. V. Role of Pt content in the microstructural development and oxidation performance of Pt–aluminide coatings produced using a high-activity aluminizing process. *Mater. Sci. Eng. A*, 1998, **251**(1-2), 40-47.
30. Johnston, G.R.; Cocking, J.L. & Johnson, W.C. A scanning Auger microscopy study of the influence of platinum on the high-temperature oxidation of a nickel-silicon-magnesium alloy. *Oxidation Metals,* 1985, **23**(5-6), 237-49.
31. de Wit, J.H.W. & van Manen, P.A. Precious metal effect in high temperature corrosion. *Mater. Sci. Forum*, 1994, **154**, 109-118.
32. Newcomb, S. B. & Stobbs, W.M. *In* Conference Proceedings on Elevated Temperature Coatings: Science and Technology II, Anaheim, California, USA, Warrendale, PA, Minerals, Metals and Materials Society 4-8 February, 1996, p. 265.
33. Allam, I.M.; Akuezue, H.C. & Whittle, D.P. Influence of small Pt additions on Al_2O_3 scale adherence. *Oxidation Metals*, 1980, **14**(6), 517-30.
34. Felten, E.J. & Petit, F.S. Development, growth, and adhesion of Al_2O_3 on platinum-aluminum alloys. *Oxidation Metals,* 1976, **10**(3), 189-223.
35. Felten, E.J. Use of platinum and rhodium to improve oxide adherence on *Ni*-8*Cr*-6*Al* alloys. *Oxidation Metals,* 1976, **10**(1), 23-28.
36. Strang, A. & Lang, E. Effect of coatings on the mechanical properties of superalloys. *In* High Temperature Alloys for Gas Turbines, edited by R. Brunetand. D. Reidel Publishing Company, Holland, 1982, pp. 469-506.

Contributors

Mr Md Zafir Alam obtained his BTech (Metallurgical Engineering) from National Institute of Technology, Rourkela and is presently pursuing his PhD from Indian Institute of Science (IISc), Bengaluru. Presently working in the Surface Engineering Group, Defence Metallurgical Research Laboratory(DMRL), Hyderabad. He has published/communicated over 15 papers in peer-reviewed journals in various national/international conferences. His research interests are development and processing of thermal barrier coatings for aero-engine and other high temperature applications, evaluating the mechanical behaviour of coated superalloys, micro-mechansims of fracture in free-standing coatings and coated superalloys.

Dr Dipak Kumar Das obtained his BTech (Hons) in Metallurgical Engineering from Indian Institute of Technology, Kharagpur and PhD from Banaras Hindu University, Banaras. Presently, he is working as Scientist 'F' at DMRL, Hyderabad. His research interests include: High temperature coatings for aeroengine, space and hypersonic applications, laser-material interaction and laser surface modification of materials, and plasma-particle interaction in plasma spray process. He has over 50 technical publications to his credit in international peer-reviewed journals.